

**High-sensitivity study of levels in  $^{30}\text{Al}$  following  $\beta$  decay of  $^{30}\text{Mg}$** 

B. Olaizola,<sup>1,\*</sup> H. Mach,<sup>1,2,3,†</sup> L. M. Fraile,<sup>1</sup> J. Benito,<sup>1</sup> M. J. G. Borge,<sup>4</sup> R. Boutami,<sup>1,4</sup> P. A. Butler,<sup>5</sup> Z. Dlouhy,<sup>6,†</sup> H. O. U. Fynbo,<sup>7</sup> P. Hoff,<sup>8</sup> S. Hyldegaard,<sup>7</sup> H. B. Jeppesen,<sup>7</sup> A. Jokinen,<sup>9,10</sup> C. Jollet,<sup>11</sup> A. Korgul,<sup>12</sup> U. Köster,<sup>13</sup> Th. Kröll,<sup>14</sup> W. Kurcewicz,<sup>12</sup> F. Marechal,<sup>11</sup> J. Mrazek,<sup>6</sup> T. Nilsson,<sup>15,16</sup> W. A. Plóciennik,<sup>3,†</sup> E. Ruchowska,<sup>3</sup> R. Schuber,<sup>17</sup> W. Schwerdtfeger,<sup>17</sup> M. Sewtz,<sup>17</sup> G. S. Simpson,<sup>18</sup> M. Stanoiu,<sup>19</sup> O. Tengblad,<sup>4</sup> P. G. Thirolf,<sup>17</sup> and D. T. Yordanov<sup>20</sup>

<sup>1</sup>*Grupo de Física Nuclear, Facultad de Físicas, Universidad Complutense - CEI Moncloa, E-28040 Madrid, Spain*

<sup>2</sup>*Department of Nuclear and Particle Physics, Uppsala University, P.O. Box 535, S-75121 Uppsala, Sweden*

<sup>3</sup>*National Centre for Nuclear Research, 04-500 Otwock-Swierk, Poland*

<sup>4</sup>*Instituto de Estructura de la Materia, CSIC, Serrano 113bis, E-28006 Madrid, Spain*

<sup>5</sup>*Oliver Lodge Laboratory, University of Liverpool, Liverpool, L69 3BX, United Kingdom*

<sup>6</sup>*Nuclear Physics Institute, AS CR, CZ-25068, Rez, Czech Republic*

<sup>7</sup>*Institut for Fysik og Astronomi, Aarhus Universitet, DK-8000 Aarhus C, Denmark*

<sup>8</sup>*Department of Chemistry, University of Oslo, P.O. Box 1033 Blindern, N-0315 Oslo, Norway*

<sup>9</sup>*University of Jyväskylä, Department of Physics, FIN-40014 Jyväskylä, Finland*

<sup>10</sup>*Helsinki Institute of Physics, P.O. Box 64, FIN-00014 Helsinki, Finland*

<sup>11</sup>*Institut de Recherches Subatomiques, IN2P3-CNRS, F-67037 Strasbourg, Cedex 2, France*

<sup>12</sup>*Faculty of Physics, University of Warsaw, PL 02-093 Warsaw, Poland*

<sup>13</sup>*Institut Laue-Langevin, B.P. 156, F-38042 Grenoble Cedex, France*

<sup>14</sup>*Institut für Kernphysik, TU Darmstadt, Schlossgartenstrasse 9 64289 Darmstadt, Germany*

<sup>15</sup>*ISOLDE, PH Department, CERN, CH-1211 Geneva 23, Switzerland*

<sup>16</sup>*Institutionen för Fysik, Chalmers Tekniska Högskola, S-412 96 Göteborg, Sweden*

<sup>17</sup>*Ludwig-Maximilians-Universität München, D-85748 Garching, Germany*

<sup>18</sup>*LPSC, Université Joseph Fourier Grenoble 1, CNRS/IN2P3, F-38026 Grenoble Cedex, France*

<sup>19</sup>*Horia Hulubei National Institute for Physics and Nuclear Engineering, P.O. Box MG-6, 077125 Bucharest-Magurele, Romania*

<sup>20</sup>*K.U. Leuven, IKS, Celestijnenlaan 200 D, 3001 Leuven, Belgium*

(Received 16 August 2016; published 21 November 2016)

$\gamma$ -ray and fast-timing spectroscopy were used to study levels in  $^{30}\text{Al}$  populated following the  $\beta^-$  decay of  $^{30}\text{Mg}$ . Five new transitions and three new levels were located in  $^{30}\text{Al}$ . A search was made to identify the third  $1^+$  state expected at an excitation energy of  $\sim 2.5$  MeV. Two new levels were found, at 3163.9 and 3362.5 keV, that are firm candidates for this state. Using the advanced time-delayed (ATD)  $\beta\gamma\gamma(t)$  method we have measured the lifetime of the 243.8-keV state to be  $T_{1/2} = 15(4)$  ps, which implies that the 243.8-keV transition is mainly of  $M1$  character. Its fast  $B(M1; 2^+ \rightarrow 3^+)$  value of 0.10(3) W.u. is in very good agreement with the USD shell-model prediction of 0.090 W.u. The 1801.5-keV level is the only level observed in this study that could be a candidate for the second excited  $2^+$  state.

DOI: [10.1103/PhysRevC.94.054318](https://doi.org/10.1103/PhysRevC.94.054318)

**I. INTRODUCTION**

In the region known as the island of inversion around  $^{32}\text{Na}$  [1], shell-model configurations are strongly rearranged. Calculations using only the  $sd$  model space fail to predict properties of these nuclei and one has to include the intruder  $pf$  orbits in their description [2]. Many studies choose to simultaneously probe nuclei outside of the island of inversion, nuclei at the transition point, and nuclei inside the region. The neutron-rich aluminum nuclei are located at an interesting

junction just at the north-western border of this special region, thus their nuclear structure is particularly challenging. This study is focused on  $^{30}\text{Al}$ , which is located just outside of the island of inversion, where in principle the shell-model calculations performed in the  $sd$  valence space should work quite well. On the other hand it is not clear to what extent the intruder  $pf$  orbits influence the structure of the excited states in this nucleus and also in the  $^{32}\text{Al}$  isotope.

There have been a number of recent studies on  $^{30}\text{Al}$  and  $^{32}\text{Al}$  probing the application of the shell-model  $sd$  valence space for the description of these nuclei. The magnetic moments of the neutron-rich aluminum isotopes, including  $^{30,31,32}\text{Al}$ , were measured by Ueno *et al.* [3,4]. The magnetic moment is an observable that is very sensitive to the orbits where the valence nucleons reside [3], and the authors found that for  $^{27-32}\text{Al}$ , the shell-model calculations using the “universal” ( $ls, 0d$ ) interaction (USD) effective interaction reproduce quite well the experimental values of magnetic moments, implying that the dominant configurations can be described within the  $sd$

\*Present address: Department of Physics, University of Guelph, Guelph, Ontario, Canada N1G 2W1; bruno.olaizola@ucm.es

†Deceased.

Published by the American Physical Society under the terms of the [Creative Commons Attribution 3.0 License](https://creativecommons.org/licenses/by/3.0/). Further distribution of this work must maintain attribution to the author(s) and the published article's title, journal citation, and DOI.

model space [4]. However, unlike for  $^{32}\text{Al}$ , for  $^{31}\text{Al}$  they have measured an electric quadrupole moment whose value is 30% lower than predicted by the model. This difference remains an enigma, since it cannot be explained by the addition of deformation driving  $pf$  configurations nor by the extended calculations within the  $sd$  model space. Nevertheless, the authors conclude that, as far as the ground-state magnetic dipole and electric quadrupole moments are concerned,  $^{30-32}\text{Al}$  are located outside of the island of inversion.

As for the low-energy structures the situation is more complicated. In particular the low-lying levels in  $^{32}\text{Al}$  represent a puzzle. The identification of a  $J^\pi = (4^+)$  200-ns isomer at 957 keV [5] created an experimental sequence of  $1^+$ ,  $2^+$ , and  $4^+$  levels that cannot be reproduced either by the shell model with  $sd$  orbits only, or by those that include also the  $pf$  configurations [5,6]. There is also evidence that the  $pf$  orbits influence the low-energy structure of heavy aluminum isotopes. Fornal *et al.* [7] have identified a new state at 1178 keV in  $^{32}\text{Al}$  that only feeds the 200-ns isomer and represents a good candidate for a  $4^-$  level arising from the intruder configurations. A  $4^-$  level at such low excitation entails a reduction in the gap between  $sd$  and  $pf$  orbits. On the other hand, an indication of a significant admixture of the intruder  $pf$  configuration in the ground state of  $^{33}\text{Al}$  was reported by Himpe *et al.* [6] based on  $g$ -factor measurements.

Hinners *et al.* [8] used the  $^{18}\text{O}(^{14}\text{C}, pn\gamma)$  reaction to search for negative-parity states in  $^{30}\text{Al}$ , which are associated with a lowering of the  $pf$  orbits. The charged particles from the reaction were detected in a  $\Delta E$ - $E$  silicon particle detector, while the  $\gamma$  rays were detected in a Compton-suppressed high-purity germanium (HPGe) array. They have identified candidates for the negative-parity states starting with a level at 2298 keV, whose possible spin-parity assignment is  $4^-$ , analogous to  $^{32}\text{Al}$ . If correct, it would represent a drop of 1.2 MeV for the  $4^-$  state when going from  $^{28}\text{Al}$  to  $^{30}\text{Al}$ . It would be also consistent with a further drop of 1.1 MeV between this state in  $^{30}\text{Al}$  and the proposed  $4^-$  state at 1178 keV in  $^{32}\text{Al}$  [7]. The study by Hinners *et al.* also encountered problems in the identification of the low-lying  $2_2^+$  and  $2_3^+$  states, since these states are strongly nonyrast. They have proposed two candidates for the  $2^+$  states, at 1562 and 1802 keV, although the experimental  $\gamma$ -ray branching ratios strongly deviate from those predicted by the shell model.

The same reaction, although in inverse kinematics, was used by Steppenbeck *et al.* [9] at the Argonne National Laboratory. Recoiling fragments were analyzed using the fragment mass analyzer [10], while the  $\gamma$  rays were detected at the target position by the Gammasphere array [11]. This study also failed to identify the negative-parity states in  $^{30}\text{Al}$  and had similar problems in identifying the  $2^+$  states. The authors found no evidence for the 1562-keV state reported in [8], but identified a new state at 2015 keV, which was then proposed as a candidate for the  $2^+$  level. The identical nuclear reaction was used by Kozub and collaborators [12] to perform  $\gamma$ -ray yield curves, angular distributions, and level lifetimes using the Doppler-shift attenuation method (DSAM) in  $^{30}\text{Al}$ . They have measured the lifetime of the 688-keV state,  $T_{1/2} = 0.7(2)$  ps, and four lifetime limits including three in the subpicosecond range. The

half-life for the 244-keV state they quote in a wide range from 2.8 ps to 8.3 ns.

The aforementioned work by Hinners *et al.* [8] also included a study on the  $\beta$  decay of  $^{30}\text{Mg}$  into the levels in  $^{30}\text{Al}$ . The aim of their work was to identify the low-lying  $1^+$  states predicted by the shell model. They observed five  $\gamma$  rays and three excited states, including a new  $1^+$  state at 2413 keV.

In the present study we use  $\gamma$ -ray and fast-timing spectroscopy to investigate levels in  $^{30}\text{Al}$  populated by the  $\beta$ -decay chain of  $^{30}\text{Na}$  [ $T_{1/2} = 49.4(20)$  ms [13]], that decays to  $^{30}\text{Mg}$  [ $T_{1/2} = 317(5)$  ms [13]] and subsequently to  $^{30}\text{Al}$  [ $T_{1/2} = 3.62(6)$  s [14]]. Our investigation takes advantage of a much higher beam intensity, which yielded  $\sim 4 \times 10^6$  detected  $^{30}\text{Al}$  photopeak events, at least 2–3 orders of magnitude higher than in previous studies. The aim is three fold: First, we intend to search for the additional  $1^+$  states in  $^{30}\text{Al}$ . Second, with the higher beam intensity and thus higher statistics, we have an opportunity to populate and study the little-known low-lying  $2^+$  states. Finally, using the advanced time-delayed (ATD)  $\beta\gamma\gamma$  method [15,16], we intend to measure the lifetime of the 243.8-keV state, which was predicted by the USD model to be  $T_{1/2} = 17$  ps [12]. Based on the close agreement between the measured values for the ground-state magnetic moments in the Al nuclei and the model predictions [3,4], one expects a good agreement also for the  $B(M1)$  transition rates. Our investigation is part of a wider fast-timing study of the  $N \approx 20$  island of inversion that was carried out at the ISOLDE facility at CERN [17].

## II. TECHNICAL ASPECTS

The activity of  $^{30}\text{Na}$  was produced at the proton-synchrotron booster (PSB) of the ISOLDE facility at CERN by bombardment of a  $45 \text{ g/cm}^2 \text{ UC}_x/\text{graphite}$  target with 1.4-GeV proton pulses from the PSB. The pulses are interspaced in multiples of 1.2 s. The  $A = 30$  ions were mass separated and deposited onto a thin aluminum stopper directly in front of a  $\beta$  detector. There was no moving-tape system to take away the decay products, thus creating a saturated source that included short- and long-lived activities coming from several radioactive decays.

The measuring station included five detectors positioned in a close geometry around the beam implantation point. The fast-timing  $\beta$  detector was a 3-mm-thick NE111A plastic scintillator placed directly behind the radioactive source. The  $\gamma$ -ray detectors included two fast-response scintillating  $\text{BaF}_2$  crystals of the Studsvik design [18] and two HPGe detectors with relative efficiency of 100%.

The experimental setup and data collection were optimized for the application of the ATD  $\beta\gamma\gamma(t)$  method described in [15,16,19], thus only a few details are given below. A time-delayed  $\beta\gamma(t)$  coincidence system was set between the  $\beta$  detector and each of the  $\gamma$  detectors and thus three parameters were required per coincident  $\beta\gamma(t)$  event: the energies of the  $\beta$  particle and the  $\gamma$  ray, and the time-delay between the  $\beta$  and  $\gamma$  events.

Triple-coincident  $\beta\gamma\gamma$  events were identified when two  $\beta\gamma(t)$  events were recorded within a time gate of 8.1  $\mu\text{s}$ . The data analysis used coincident events collected in the

$\beta$ -HPGe-HPGe or  $\beta$ -HPGe-BaF<sub>2</sub> combination of detectors. These sets allowed identification of  $\gamma$  rays observed in the spectra and the construction or verification of the level scheme. Moreover, it allowed the identification of  $\gamma$  rays present in the coincident BaF<sub>2</sub> energy spectra characterized by much worse energy resolution than HPGe spectra. The HPGe detectors were calibrated using  $^{24}\text{Na}$ ,  $^{88}\text{Rb}$ , and  $^{140}\text{Ba}/^{140}\text{La}$ , off-line sources. This calibration was further verified using the most intense  $\gamma$  lines in  $^{30}\text{Si}$  from the experiment.

In the ATD method [15,16,19] the time responses of the fast-timing  $\gamma$  detectors (BaF<sub>2</sub> crystals with a FWHM time resolution around 100 ps at 1 MeV) are carefully calibrated (to a picosecond precision) for various types of interactions of  $\gamma$  rays in the crystal (Compton and full energy peak (FEP) events). It is also checked that the shape of time spectra for prompt radiation is close to symmetric quasi-Gaussians over the range of the  $\gamma$ -ray energies of interest. In particular, time-walk (the energy dependence of the time response) calibrations of the BaF<sub>2</sub> detectors were obtained off-line using sources of  $^{24}\text{Na}$ ,  $^{88}\text{Rb}$  and  $^{140}\text{Ba}/^{140}\text{La}$ .

### III. RESULTS ON $^{30}\text{Al}$

For the analysis, data were prepared by selecting a time gate of 300–1200 ms after the proton impact. This allowed the  $^{30}\text{Na}$  to decay away and enhanced the  $^{30}\text{Mg}$  activity (see Fig. 1). The identification of  $\gamma$  transitions in  $^{30}\text{Al}$  from the  $\beta$  decay of  $^{30}\text{Mg}$  was done based on the time behavior of the activity (see below) and on coincidences with already known transitions. As an example the HPGe energy spectrum in coincidence with the strongest 243.8-keV transition is shown in Fig. 2. Together with the most intense coincident  $\gamma$  lines, smaller peaks are visible with sufficient statistics.

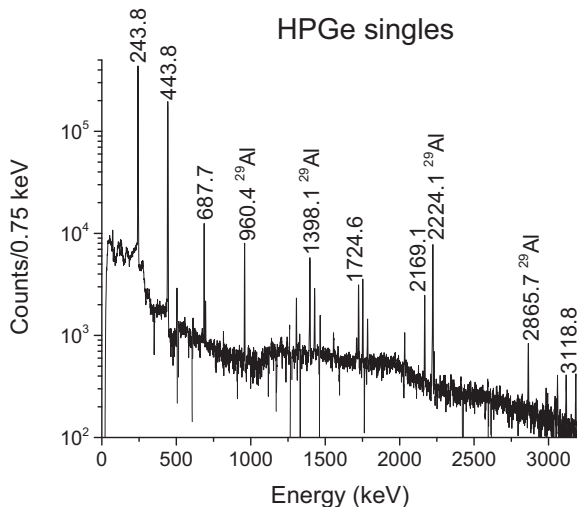


FIG. 1. HPGe singles energy spectrum, with  $^{30}\text{Al}$  peaks identified. A time gate of 300–1200 ms after the proton impact on target was selected to enhance the  $^{30}\text{Mg}$  activity. In this time range the  $^{30}\text{Na}$  has decayed away. In a second step, the  $^{30}\text{Al}$  decay to  $^{30}\text{Si}$  was subtracted. This did not suppress the  $^{29}\text{Al}$  peaks (the  $A = 29$  chain was present in the experiment due to the  $\beta$ - $n$  branch in  $^{30}\text{Na}$  [13]) but oversubtracted the peaks in  $^{29}\text{Si}$ .

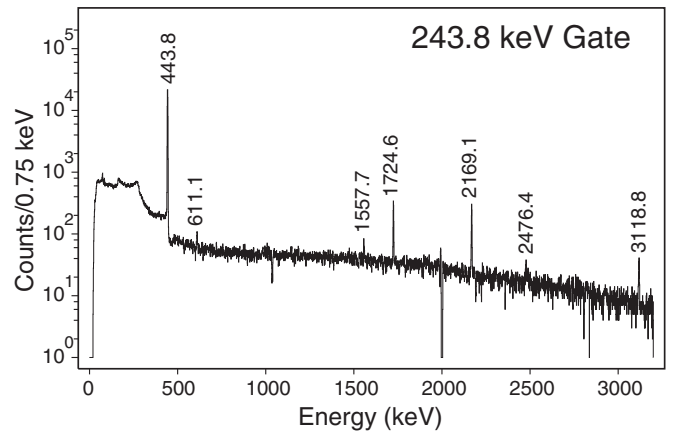


FIG. 2. HPGe-HPGe coincidences energy spectrum with a condition on the 243.8-keV transition.

The data acquisition system employed in the experiment suffered from severe dead time, as can be seen in Fig. 3. This problem was tracked down to the writing of data buffers and it was corrected during the off-line analysis (black dots in Fig. 3). The correction was done by multiplying the time spectra by the dead-time-to-live-time ratio as a function of the time since proton impact. The goodness of this correction was cross-checked by satisfactorily fitting the various half-lives of the isotopes down the decay chain. The  $^{30}\text{Al}$  was fitted to obtain the half-life of  $^{30}\text{Mg}$  using the time reference of the proton beam impacting on the target. The fit yielded  $T_{1/2} = 335(10)$  ms. The statistical error was below 1 ms, but a systematic error of 10 ms was introduced to account for uncertainties in the correction of the dead time. Nevertheless different fits were performed varying the fit range and binning and the results were found to be very consistent, well below the conservative 10-ms systematic error. Our result seems to

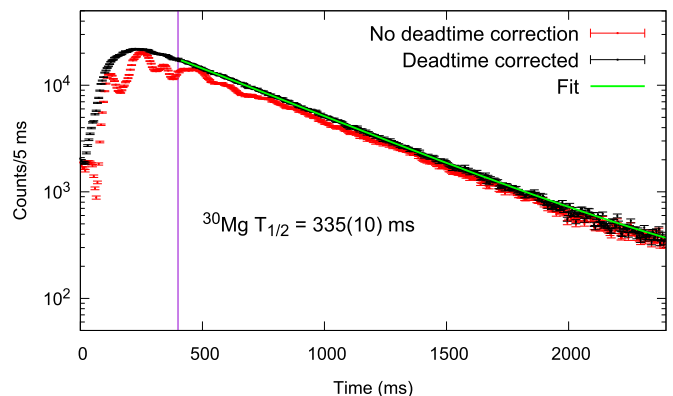


FIG. 3.  $^{30}\text{Al}$  activity gated on the 243.8-keV transition. The red (gray) dots show the activity before the dead-time correction and the black dots after the off-line correction. The green (light gray) line is a fit to the dead-time-corrected activity and the purple vertical line shows the fitting-range limit. The Bateman equation for a decay chain [20] was used for the fit, with the half-life of  $^{30}\text{Na}$  [ $T_{1/2} = 49.4(20)$  ms [13]] as a fixed parameter and a constant background, a normalization factor, and the  $^{30}\text{Mg}$  half-life as free ones.

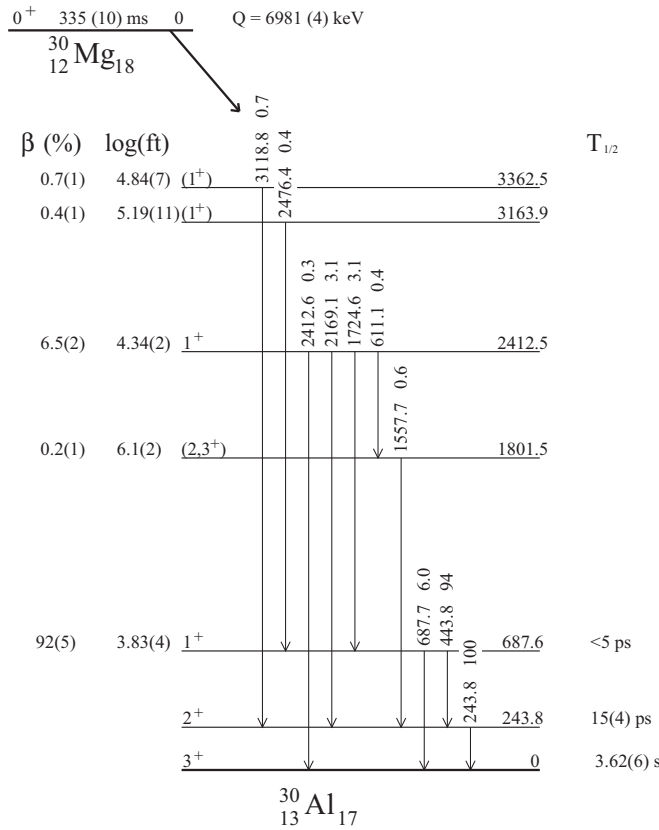


FIG. 4. Partial level scheme of  $^{30}\text{Al}$  populated following the  $\beta^-$  decay of  $^{30}\text{Mg}$  from this work. For absolute intensity per 100 decays, multiply by 0.94(5).  $Q_\beta$  value was obtained from [24].

fit better with older results (see compilation in Ref. [13]) than with the  $T_{1/2} = 316(5)$  ms obtained by Hinners *et al.* [8], but they still agree within  $2\sigma$ .

Figure 4 shows the level scheme of  $^{30}\text{Al}$  populated in the  $\beta^-$  decay of  $^{30}\text{Mg}$  observed during this experiment. The 243.8(1)-, 687.6(1)- and 2412.5(1)-keV levels were already observed in [8,21,22] and the energies are in good agreement. Steppenbeck *et al.* [9] reported levels at 242.9(1), 685.7(1), and 1798.0(5) keV populated in the  $^{14}\text{C}(^{18}\text{O}, pn\gamma)$  reaction. We observe these levels in our level scheme, but at systematically higher energy, and well beyond the  $1\sigma$  error bar. Conversion electrons were deemed negligible for all transitions [23]. No direct feeding of the  $^{30}\text{Al}$  ground state was assumed, due to the  $\Delta J = 3$  difference between the parent and daughter ground states.

Using the centroid shift technique described in Ref. [15] the mean lifetime of the 243.8-keV level was measured. Because the experiment employed two fast crystals, the value was measured independently twice, both in perfect agreement:  $\tau_1 = 22(8)$  and  $\tau_2 = 21(8)$  ps. For an example of a time spectrum of one of the crystals, see Fig. 5. The final result is given as a weighted average of the two values,  $T_{1/2} = 15(4)$  ps. Since the statistics for both the  $^{30}\text{Al}$  data and the calibration is very high, the main source of error comes from the uncertainty in the lifetimes in the  $^{140}\text{La}$  calibration source employed. It has to be noted that the half-life of the 467.6-keV level in

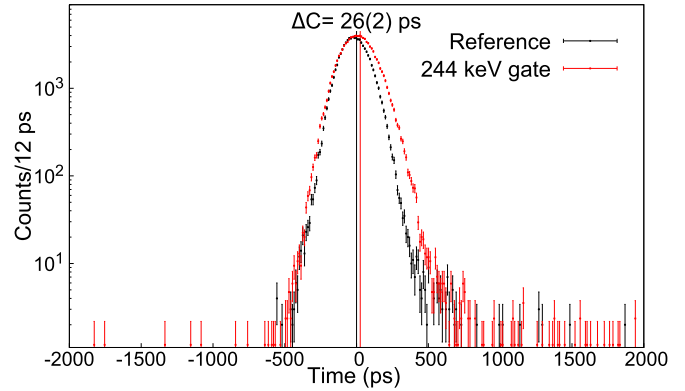


FIG. 5. Time difference of the  $\beta - \text{BaF}_2(t)$  coincidence with a gate on the 243.8-keV transition, shown for the second  $\text{BaF}_2$ . To precisely select a particular  $\gamma$ -cascade decay, an additional coincidence with the 443.8-keV transition was made with the HPGe detectors. To obtain the final  $\tau = 21(8)$  ps, the centroid shift  $\Delta C$  shown must be corrected by the energy-dependent time walk of the  $\text{BaF}_2$  crystal,  $-7(7)$  ps in this case, and the Compton contribution,  $+2(1)$  ps.

$^{140}\text{La}$  is  $T_{1/2} < 7.7$  ps [25] and not  $T_{1/2} < 7.7$  ns, as it is wrongly quoted in the database [26]. A pure  $M1$  character for the 243.8(1)-keV transition was already determined by the fit of the angular distribution [8], which with the new experimental half-life yields  $B(M1) = 0.10(3)$  W.u. (Table I). This transition rate is of the same order of magnitude as that of other reported  $M1$  transitions in  $^{30}\text{Al}$  measured in nuclear reactions (see Table II in Ref. [12]).

By employing the parallel transitions technique (for a detailed explanation see [15]), it was possible to set an upper limit to the lifetime of the 687.6-keV level. Two time spectra were generated. In one of them the 2169.1-keV transition was selected in the HPGe detector. In the other one this detector had a condition on the 1724.6-keV line. Both spectra had an energy gate on the 243.8-keV transition in the  $\text{BaF}_2$  crystals. From the difference of the centroids of both time distributions an upper limit of  $<5$  ps for the 687.6-keV level was obtained. This limit is consistent with the  $T_{1/2} = 0.7(2)$  ps result from [12], a value that is below the precision of the current experiment. Table I shows the limits for the reduced transition probabilities for transitions depopulating this level.

The level found at 1801.5 keV in this work has been observed in  $\beta$  decay for the first time, but most likely it can be identified as the 1802-keV state observed in the  $^{18}\text{O}(^{14}\text{C}, pn\gamma)$  reaction [8], and in the same reaction but in inverse kinematics at 1798.0(5) in [9]. It presents a negligible  $\beta$  feeding, which suggests a spin of 2 or higher. It is populated by the 611.1-keV transition from the  $1^+$  state above it, so spins higher than 3 can be discarded. We tentatively propose a spin-parity of  $(2,3)^+$  for this level. Negative-parity assignments have not been considered for this level because shell-model calculations do not predict any  $1^-$  states below 3.5 MeV nor a  $2^-$  state below 2.5 MeV (see Refs. [8,9]). Hinners *et al.* were not able to perform angular correlations on the 1802-keV level, but they identified it as the  $2_3^+$  state predicted by the calculations

TABLE I. Levels, transitions, lifetimes, and reduced transition probabilities measured in  $^{30}\text{Al}$ , see text for details. The transition relative intensity has been normalized to 100 for the 243.8-keV  $\gamma$  ray. The  $\dagger$  indicates levels and transitions seen for the first time in this work. The \* indicates levels and transitions not seen previously in  $\beta$  decay but observed in nuclear reactions at similar energies.

| Initial level (keV)    | $J^\pi$   | $T_{1/2}$<br>This work<br>(ps) | $T_{1/2}$<br>Other works   | $E_\gamma$<br>(keV)    | $I_\gamma$          | $J_f^\pi$<br>Final level | $E_M \lambda$ | $B_{\text{expt}}(E_M \lambda)$<br>(W.u.) |
|------------------------|-----------|--------------------------------|----------------------------|------------------------|---------------------|--------------------------|---------------|--|
| 0.0                    | $3^+$     |                                | 3.62 s                     |                        |                     |                          |               |  |
| 243.8(1)               | $2^+$     | 15(4)                          | $<8 \text{ ns}^{\text{a}}$ | 243.8(1)               | 100                 | $3^+$                    | $M1$          | 0.10(3)                                  |
| 687.6(1)               | $1^+$     | $<5$                           | 0.7(1) ps <sup>b</sup>     | 687.7(1)               | 94(6)               | $2^+$                    | $M1$          | $>4.7 \times 10^{-2}$                    |
|                        |           |                                |                            | 687.7(1)               | 6.0(3)              | $3^+$                    | $E2$          | $>7.8$                                   |
| 1801.5(2)*             | $(2,3)^+$ |                                |                            | 1557.7(2)*             | 0.6(1)              | $2^+$                    |               |  |
| 2412.5(2)              | $1^+$     |                                |                            | 611.1(6) <sup>†</sup>  | 0.4(1) <sup>c</sup> | $(2,3)^+$                |               |  |
|                        |           |                                |                            | 1724.6(2)              | 3.1(4) <sup>c</sup> | $1^+$                    |               |  |
|                        |           |                                |                            | 2169.1(1)              | 3.1(3)              | $2^+$                    |               |  |
|                        |           |                                |                            | 2412.6(3) <sup>†</sup> | 0.3(1)              | $3^+$                    |               |  |
| 3163.9(4) <sup>†</sup> | $(1^+)$   |                                |                            | 2476.4(3) <sup>†</sup> | 0.4(1)              | $1^+$                    |               |  |
| 3362.5(2) <sup>†</sup> | $(1^+)$   |                                |                            | 3118.8(2) <sup>†</sup> | 0.7(1)              | $2^+$                    |               |  |

<sup>a</sup>Private communication [27] in evaluation [28].

<sup>b</sup>Lifetime from Ref. [12].

<sup>c</sup>Intensity obtained from coincidences spectra.

just based on the similarity of energies, despite the total disagreement in the branching ratios.

The two newly identified levels in this work, at 3163.9 and 3362.5 keV, have  $\log(ft)$  values of 5.19(11) and 4.84(7) respectively. According to Ref. [29], the feeding to the  $1_1^+$  state at 687.6 keV exhausts almost all the  $\beta$ -decay strength. This and their high energy make it very unlikely that any unobserved  $\gamma$  transitions populate them from above with significant intensity. Because of this direct  $\beta$  feeding, these two levels are tentatively assigned as new  $(1^+)$  states.

By using the intensity of all the  $\gamma$  rays directly populating the ground state we calculated a normalization factor of 0.94(5) (again, no direct  $\beta$  feeding was assumed for the ground state). This result does not agree with the value of 0.74(10) calculated in the compilation [28], most likely obtained from an older  $\beta$ -decay work on the region [22]. Our normalization factor can be favorably compared to that obtained by Hinners *et al.* of 0.98(3) [8].

#### IV. DISCUSSION

The experimental results have been compared with the available shell-model calculations for this region. Li and Ren [30] performed shell-model calculations based on the Warburton-Seeker-Millener-Brown (WBMB) interaction [31] to predict the  $^{30}\text{Mg}$  decay properties. For nuclei with  $N \leq 20$  they used the  $\pi(1s,0d)\nu(1s,0d,0f_{7/2})$  valence space, but they noticed that a larger space should be used to improve the predictions of the region. They predicted a 286-ms half-life, which compares well to our result of 335(10) ms. They also calculated a  $P_n = 0.00\%$  for the  $\beta$ -delayed neutron emission branch. Although compilations quote  $P_n \leq 0.06\%$  [13], they seem to have overlooked that Hinners and collaborators [8] observed the presence of  $^{29}\text{Al}$  transitions in their experiment and gave a  $P_n > 2\%$  limit. Even if our experiment does not have the precision to give a  $P_n$  value (mainly because

of the  $^{30}\text{Na}$   $P_n = 30(5)\%$  branch [13]), it seems to hint of the presence of a non-negligible  $^{30}\text{Mg}$   $\beta$ -delayed neutron emission branch.

Last, in Ref. [30] the direct  $\beta$  population of the first two  $1^+$  states was calculated. They obtained these levels at 470 and 2109 keV, measured at 687.6 and 2412.5 keV in this experiment. They calculated  $\log(ft)=3.832$  and 4.339 for them, which are in excellent agreement with the 3.83(4) and 4.34(2) values obtained in this work, as well as branching ratios of 91.01% and 7.45%, compared to our 92(5)% and 6.5(2)% measured ones. Kozub *et al.* [12] calculated electromagnetic transition rates in  $^{30}\text{Al}$ , obtaining  $B(M1) = 0.090$  W.u. for the 243.8-keV transition. This compares very well to the  $B(M1) = 0.10(3)$  W.u. measured in the present work.

Hinners *et al.* (Fig. 12 in Ref. [8]) and Steppenbeck *et al.* (Fig. 6 in Ref. [9]) both published predictions of shell-model calculations using the USD, USDA, and USDB effective interactions for the  $^{30}\text{Al}$  nuclear structure with identical results. The calculations are able to reproduce the positive-parity state ordering, even if the energies seem to be systematically lower. All three interactions (USD, USDA, and USDB) obtain the  $1_3^+$  state at  $\sim 2.5$  MeV, which could be matched to the newly observed state at 3163.9 keV. They both seem to calculate only the three first states for each angular momentum, so no  $1_4^+$  is shown for comparison with the observed state at 3362.5 keV.

The  $\beta$  population and decay pattern of the 1801.5-keV level do not allow spins of  $2^+$  and  $3^+$  to be distinguished. The calculations predict the  $3_2^+$  at  $\sim 800$ – $900$  keV, but that state has been identified as the 1117–1120-keV level in nuclear reactions and no level is populated in  $\beta$  decay near that energy. The next  $3_3^+$  state is calculated to have an energy of about 2.5–2.8 MeV. The  $2_2^+$  and  $2_3^+$  states are predicted to lie between 1.3 and 2.0 MeV (depending on the interaction employed). This scenario seems to favor the  $(2^+)$  spin for the 1801.5-keV level, but no firm assignment can be made based on the experimental results. In their work Hinners *et al.* [8] seem to favor also this assignment over the  $3^+$ ,

even if they acknowledged essentially no agreement with the calculated branching ratios. Steppenbeck and collaborators [9] also suggest a ( $2^+$ ) spin assignment based on shell-model calculations for their state at 1798 keV (which they match to the one at 1802 keV in Ref. [8]) and claim a better agreement with the theoretically predicted branching ratios. They observed a transition between this state and the  $1_1^+$  at 687.6 keV of  $\sim 1113$  keV,  $\sim 10$  times weaker than the transition from this level to the  $2_1^+$  state. We have made a dedicated search for a 1113.9-keV transition (according to the energy difference of the states seen in this work) connecting the 1801.5-keV level to the 687.6-keV state, but if it exists its intensity is below our sensitivity limit of 0.05 units at this energy. Shell-model calculations predict a more intense transition from the  $2_2^+$  to the ground state, but it has not been observed either in this or in previous works.

## V. CONCLUSIONS

$\gamma$ -ray and fast-timing spectroscopy were used to study levels in  $^{30}\text{Al}$  populated following the  $\beta^-$  decay of  $^{30}\text{Mg}$ . Our present work verifies the known level scheme of  $^{30}\text{Al}$  with increased precision. Furthermore, we have expanded it with five new transitions and three new levels not seen previously in  $\beta$  decay, for which tentative spins and parities have been assigned. Two new levels were observed for the first time, at 3163.9 and 3362.5 keV, that are firm candidates to be  $1^+$  states, expected at this excitation energy. Using the ATD  $\beta\gamma\gamma(t)$  method, the lifetime of the first excited state at 243.8 keV has been measured for the first time to be  $T_{1/2} = 15(4)$  ps.

An upper limit has been set for the half-life of the second excited state, consistent with the previously reported value. The 1801.5-keV level is the only one observed in this study that could be a candidate for the second excited  $2^+$  state, but discrepancies with the predicted  $\gamma$  branching ratios still remain.

The measured  $B(M1)$  transition rates, in perfect agreement with the shell-model calculations using only a full  $sd$  model space, confirm that  $^{30}\text{Al}$  is indeed outside the island of inversion and no significant occupation of the  $pf$  intruder orbits is required to describe the low-lying positive-parity states. This is further supported by the finding in this work of the predicted  $1_3^+$  state, in relatively good agreement with the calculated energy.

## ACKNOWLEDGMENTS

We would like to acknowledge our colleague Henryk Mach, who recently passed away, for his invaluable contributions to the field of  $\beta$  decay and fast-timing spectroscopy. We appreciate not only his outstanding scientific work, but also his tireless effort as our mentor. He will be sorely missed.

Fast-timing detectors and electronics were provided by the Fast Timing Collaboration. This work was supported in part by the Spanish MINECO through the FPA2013-41467-P, FPA2015-64969-P, and FPA2015-65035-P projects, Grupo de Física Nuclear (GFN) at UCM and by the NuPNET network FATIMA via the PRI-PIMNUP-2011-1338 project. Support by the European Union Sixth Framework Programme through RII3-EURONS (Contract No. 506065) is acknowledged.

- 
- [1] C. Thibault, R. Klapisch, C. Rigaud, A. M. Poskanzer, R. Prieels, L. Lessard, and W. Reisdorf, *Phys. Rev. C* **12**, 644 (1975).
  - [2] X. Campi, H. Flocard, A. Kerman, and S. Koonin, *Nucl. Phys. A* **251**, 193 (1975).
  - [3] H. Ueno, D. Kameda, G. Kijima, K. Asahi, A. Yoshimi, H. Miyoshi, K. Shimada, G. Kato, D. Nagae, S. Emori, T. Haseyama, H. Watanabe, and M. Tsukui, *Phys. Lett. B* **615**, 186 (2005).
  - [4] H. Ueno, D. Kameda, D. Nagae, M. Takemura, K. Asahi, K. Shimada, K. Takase, T. Sugimoto, T. Nagatomo, M. Uchida, T. Arai, T. Inoue, A. Yoshimi, T. Kawamura, and K. Narita, *Eur. Phys. J. ST* **150**, 185 (2007).
  - [5] M. Robinson, P. Halse, W. Trinder, R. Anne, C. Borcea, M. Lewitowicz, S. Lukyanov, M. Mirea, Y. Oganessian, N. A. Orr, Y. Penionzhkevich, M. G. Saint-Laurent, and O. Tarasov, *Phys. Rev. C* **53**, R1465 (1996).
  - [6] P. Himpe, G. Neyens, D. Balabanski, G. Bfler, D. Borremans, J. Daugas, F. de Oliveira Santos, M. D. Rydt, K. Flanagan, G. Georgiev, M. Kowalska, S. Mallion, I. Matea, P. Morel, Y. Penionzhkevich, N. Smirnova, C. Stodel, K. Turzó, N. Vermeulen, and D. Yordanov, *Phys. Lett. B* **643**, 257 (2006).
  - [7] B. Fornal, R. Broda, W. Królas, T. Pawlat, J. Wrzesiński, D. Bazzacco, D. Fabris, S. Lunardi, C. Rossi Alvarez, G. Viesti, G. de Angelis, M. Cinausero, D. R. Napoli, and Z. W. Grabowski, *Phys. Rev. C* **55**, 762 (1997).
  - [8] T. A. Hinnners, V. Tripathi, S. L. Tabor, A. Volya, P. C. Bender, C. R. Hoffman, S. Lee, M. Perry, P. F. Mantica, A. D. Davies, S. N. Liddick, W. F. Mueller, A. Stolz, and B. E. Tomlin, *Phys. Rev. C* **77**, 034305 (2008).
  - [9] D. Steppenbeck, A. Deacon, S. Freeman, R. Janssens, M. Carpenter, C. Hoffman, B. Kay, T. Lauritsen, C. Lister, D. O'Donnell, J. Ollier, D. Seweryniak, J. Smith, K.-M. Spohr, S. Tabor, V. Tripathi, P. Wady, and S. Zhu, *Nucl. Phys. A* **847**, 149 (2010).
  - [10] C. N. Davids and J. D. Larson, *Nucl. Instrum. Methods Phys. Res., Sect. B* **40**, 1224 (1989).
  - [11] I.-Y. Lee, *Nucl. Phys. A* **520**, c641 (1990).
  - [12] R. L. Kozub, C. B. Chitwood, D. J. Fields, C. J. Lister, J. W. Olness, and E. K. Warburton, *Phys. Rev. C* **28**, 2343 (1983).
  - [13] M. Birch, B. Singh, I. Dillmann, D. Abriola, T. Johnson, E. McCutchan, and A. Sonzogno, *Nucl. Data Sheets* **128**, 131 (2015).
  - [14] National Nuclear Database Center, Information extracted from the Chart of Nuclides database.
  - [15] H. Mach, R. Gill, and M. Moszyński, *Nucl. Instrum. Methods Phys. Res., Sect. A* **280**, 49 (1989).
  - [16] M. Moszyński and H. Mach, *Nucl. Instrum. Methods Phys. Res., Sect. A* **277**, 407 (1989).
  - [17] H. Mach, L. Fraile, O. Tengblad, R. Boutami, C. Jollet, W. Płóciennik, D. Yordanov, M. Stanoiu, M. Borge, P. Butler,

- J. Cederkäll, P. Dessagne, B. Fogelberg, H. Fynbo, P. Hoff, A. Jokinen, A. Korgul, U. Köster, W. Kurcewicz, F. Marechal, T. Motobayashi, J. Mrazek, G. Neyens, T. Nilsson, S. Pedersen, A. Poves, B. Rubio, and E. Ruchowska, *Eur. Phys. J. A* **25**, 105 (2005).
- [18] H. Mach and L. Fraile, *Hyperfine Interact.* **223**, 147 (2014).
- [19] H. Mach, F. Wohn, G. Molnár, K. Sistemich, J. C. Hill, M. Moszyński, R. Gill, W. Krips, and D. Brenner, *Nucl. Phys. A* **523**, 197 (1991).
- [20] H. Bateman, *Proc. Camb. Phil. Soc.* **16**, 423 (1910).
- [21] C. Détraz, D. Guillemaud, G. Huber, R. Klapisch, M. Langevin, F. Naulin, C. Thibault, L. C. Carraz, and F. Touchard, *Phys. Rev. C* **19**, 164 (1979).
- [22] D. Guillemaud-Mueller, C. Detraz, M. Langevin, F. Naulin, M. de Saint-Simon, C. Thibault, F. Touchard, and M. Epherre, *Nucl. Phys. A* **426**, 37 (1984).
- [23] T. Kibédi, T. W. Burrows, M. B. Trzhaskovskaya, P. M. Davidson, and C. W. Nestor, *Nucl. Instrum. Methods Phys. Res., Sect. A* **589**, 202 (2008).
- [24] A. A. Kwiatkowski, C. Andreoiu, J. C. Bale, A. Chaudhuri, U. Chowdhury, S. Malbrunot-Ettenauer, A. T. Gallant, A. Grossheim, G. Gwinner, A. Lennarz, T. D. Macdonald, T. J. M. Rauch, B. E. Schultz, S. Seeraji, M. C. Simon, V. V. Simon, D. Lunney, A. Poves, and J. Dilling, *Phys. Rev. C* **92**, 061301 (2015).
- [25] J. Burde, M. Rakavy, and G. Adam, *Nucl. Phys.* **68**, 561 (1965).
- [26] N. Nica, *Nucl. Data Sheets* **108**, 1287 (2007).
- [27] D. Steppenbeck, A. N. Deacon, S. J. Freeman, R. V. F. Janssens, M. P. Carpenter, C. R. Hoffman, B. P. Kay, T. Lauritsen, C. J. Lister, D. O'Donnell, J. Ollier, D. Seweryniak, J. F. Smith, K. M. Spohr, S. L. Tabor, V. Tripathi, P. T. Wady, and S. Zhu (private communication).
- [28] M. S. Basunia, *Nucl. Data Sheets* **111**, 2331 (2010).
- [29] O. Sorlin and M.-G. Porquet, *Prog. Part. Nucl. Phys.* **61**, 602 (2008).
- [30] H. Li and Z. Ren, *J. Phys. G: Nucl. Part. Phys.* **40**, 105110 (2013).
- [31] E. K. Warburton, J. A. Becker, and B. A. Brown, *Phys. Rev. C* **41**, 1147 (1990).